Brown, B.S., et al., 2022, Unleashing alkali feldspar: Ra/Th ages and chemical and isotopic constraints on Holocene phonolite magmatism, Canary Islands: Geology, v. 50, https://doi.org/10.1130/G50112.1

SUPPLEMENTAL MATERIAL

SAMPLES, PREPARATION, AND ANALYTICAL METHODS

Three phonolitic lavas (Fig. 1) were collected from within Las Cañadas caldera, and one phonolitic lava (Teide H) was collected ~5 km northwest of the northern caldera flank (Table 1). Lavas (Fig. DR1) were crushed using a mortar and pestle and sieved into >1 mm, 1 mm – 355 μm, 354 μm – 250 μm, and <250 μm sizes. Alkali feldspar crystals and crystal fragments >355 μm were separated, etched in 10% hydrofluoric acid in 20-minute intervals, and sonicated for 30 minutes to remove any adhering volcanic glass or groundmass (note etching left feldspars intact). Individual feldspar crystals or crystal fragments ranging from 0.4 mg to 8.9 mg were hand picked to exclude visible melt or mineral inclusions (Fig. DR2). Feldspar separates composed of >20 individual crystals or crystal fragments <1 mg each were also prepared from three of the lavas processed.

In addition to crystals, groundmass fragments >355 μm were hand picked and preferentially chosen to avoid visible crystalline material in an effort to best obtain a sample of melt. Prior to separation, groundmass fractions were leached in 0.25 N HCl for ~20 minutes to remove any precipitants on grain surfaces, including seawater precipitated salts. Following cleaning, ~150 mg of groundmass from each sample was isolated for processing.

Crystal-free groundmass, feldspar separates, and single feldspar crystals/fragments were dissolved either directly or using a sequential digestion process and Ca, Sr, Ba, U, Th, Ra, and Pb concentrations or isotope ratios were determined using isotope dilution methods. Feldspar separates and single feldspar crystals/fragments were dissolved directly using doubly-distilled hydrofluoric, nitric, and hydrochloric acids. Groundmass separates were initially dissolved using 2% hydrofluoric acid in one-hour, sequential steps to avoid digestion of mineral grains or grain

fragments remaining in the crystal-free separate. After sequential digestion, the groundmass was dissolved using doubly-distilled hydrofluoric, nitric, and hydrochloric acids. Digested solutions of groundmass and feldspar were split into aliquots for Ca/Ba, U/Th, Rb/Sr, and Ra concentration measurements. Additional splits were made for Sr, Pb, and Nd (groundmass only) isotope measurements. Elemental purifications used cation, anion, and HDEHP resins following Ramos and Tepley (2008), Ramos and Rosenberg (2012), and Ramos et al. (2016).

Purified Rb and Sr samples were analyzed using thermal ionization mass spectrometry (TIMS) and purified Ca, Ba, Nd, Pb, U, Th, and Ra were analyzed using multi-collector inductively coupled plasma mass spectrometry (MC-ICP-MS) at New Mexico State University (Tables DR1, DR2, and DR3). Concentration accuracies were estimated to be ≤2% for all concentration measurements and mixed Ca/Ba and Rb/Sr spikes were calibrated to BCR-C (CaO=6.98 wt%, Ba=685 ppm, and Sr=335 ppm), an analog rock powder of USGS BCR1. Alkali feldspar partition coefficients of Ca, Sr, and Ba were then calculated using elemental concentrations of crystals and the groundmass (i.e., melt). Measurement sensitivities for all elements analyzed were below the analyte amounts measured. Only feldspars ≤0.5 mg approached our limits of radium detection.

Feldspars were analyzed with a JEOL JXA8500F Field Emission Electron Microprobe at the Peter Hooper GeoAnalytical Lab of Washington State University (Fig. DR3; Table DR5). All data were acquired and reduced with Probe For EPMA (PFE). Analytical conditions were 15 kV accelerating voltage, 15 nA current, and a 5 μm beam diameter. Mean Atomic Number background estimates were used for all elements, except Al and Si, which were acquired using EDS, and processed through PFE with full standardization and matrix corrections. Average relative uncertainties are Si=0.6%, Al=1%, Ca=1.7%, Na=0.8%, and K=0.9%.

FELDSPAR AGE CALCULATIONS

Single feldspar crystals/fragments and feldspar separate ages were determined using procedures described in Ramos et al. (2019), which rely on predicting D_{Ra} using the lattice strain model (Blundy and Wood, 1994). A model parabola was fit to the D_{Ca}, D_{Sr}, and D_{Ba} determinations for each individual feldspar or feldspar separate when plotted against the respective cation radii of Ca^{2+}, Sr^{2+}, and Ba^{2+} (Figs. DR4–7). The shape ('tightness') of each parabola, corresponding to the cation site elastic modulus E, was assessed. Values for E for divalent cations derived from alkali feldspar/melt partitioning experiments (Long, 1978; Icenhower and London, 1996; Fabbrizio et al., 2009) lie in the range 120 ± 40 GPa, and most of our results are within this range. Results lying outside this range giving discrepant values of D_{Ra}/D_{Ba} (Table DR2) were rejected along with those not yielding parabolic Onuma curves (see main text). D_{Ra} was assumed to lie at the intersection of the parabola with the cation size of Ra^{2+} (1.48 Å). Once D_{Ra} and D_{Ra}/D_{Ba} were known, the present-day groundmass and feldspar radium concentrations were separately age corrected for ^{226}Ra decay or ingrowth in the past to obtain the D_{Ra} or the D_{Ra}/D_{Ba} ratio at crystallization for each individual feldspar or feldspar separate. An example of the curves representing the ^{226}Ra concentrations of the melt and the feldspar in the past are presented in Fig. DR8. For the melt, which was radium depleted (i.e., $(^{226}Ra)/(^{230}Th)<1.0$), ^{226}Ra decay and ^{226}Ra ingrowth from ^{230}Th occurred with time. For feldspar, in which Th is incompatible, only ^{226}Ra decay occurred with time. Prior to age correcting, feldspar ^{226}Ra concentrations were corrected for melt inclusions that hosted ^{226}Ra assuming that the melt inclusions had the same radium concentrations as the host melt at eruption. Note, all feldspars had ≤3.6% melt inclusions by volume so any radium present in melt inclusions had little impact on young crystals but larger impacts on older crystals with less

radium (e.g., Arenas Blancas feldspar radium concentrations reflected a ~6% radium contribution from ~1% MIs in a ~4 ka feldspar, while ~1 ka feldspars in Lavas Negras had a <1% radium contribution resulting from a ~1% melt inclusion volume). Most corrections were much smaller than the errors associated with individual feldspar ages. The specific age in the past which yielded the appropriate D_{Ra}/D_{Ba} for each feldspar or feldspar separate was then chosen as the feldspar age of crystallization. Additionally, we note that temperatures (~850°C; Andújar and Scaillet, 2012) for Tenerife phonolites would only allow for minimal radium diffusion with little impact on resulting feldspar ages (Ramos et al., 2019).

FELDSPAR AGE VARIATIONS RESULTING FROM LATE-STAGE ASSIMILATION

Model Onuma curves were generated to evaluate the impact of late-stage assimilation affecting Sr concentrations occurring after feldspar crystallization in the Arenas Blancas melt (i.e., groundmass) on D_{Ra}/D_{Ba} of feldspar and ultimately on calculated feldspar crystallization ages. In the Arenas Blancas lava, three phenocrysts (K2–K4) have ages of ~4 ka but the groundmass has more radiogenic $^{87}Sr/^{86}Sr$ than these crystals (~0.7035 vs. ~0.7031) consistent with late-stage assimilation. Given that the measured Sr concentration of the groundmass is 8 ppm, we have undertaken modeling to determine feldspar phenocryst ages if we assume 2 ppm (25%) and 4 ppm (50%) of the total Sr results from assimilation. Overall, we view this as unlikely given that the assimilation-affected, Arenas Blancas groundmass has an $^{87}Sr/^{86}Sr$ ratio of 0.7035 and any potential assimilant would likely be affected by seawater, which has $^{87}Sr/^{86}Sr$ of ~0.7092. Model Onuma curves for the 25% Sr assimilation contribution (8 ppm: D_{Sr}=15.4 to 6 ppm: D_{Sr}=20.5), yield calculated feldspar ages that are ~150 years younger. For the 50% Sr assimilation contribution (8 ppm: D_{Sr}=15.4 to 4 ppm: D_{Sr}=30.8), the calculated ages were ~500 years younger or just outside the estimated error of 10% (~400 years) for the original ~4 ka age.

Given the unlikelihood that half of the Sr in the groundmass originates from assimilation (i.e., the $^{87}Sr/^{86}Sr$ is only ~0.7035), we view feldspar ages as robust despite minor, late-stage assimilation. Note also that assimilation is likely to affect Sr and $^{87}Sr/^{86}Sr$ ratios more than accompanying divalent ions (i.e., Ca and Ba) because Sr is extraordinarily depleted in phonolite groundmass.

98 Figure DR1. Images of hand samples processed for alkali feldspar and groundmass for the A)

99 Lavas Negras, B) Montaña Blanca, C) Arenas Blancas, and D) Teide H flows.

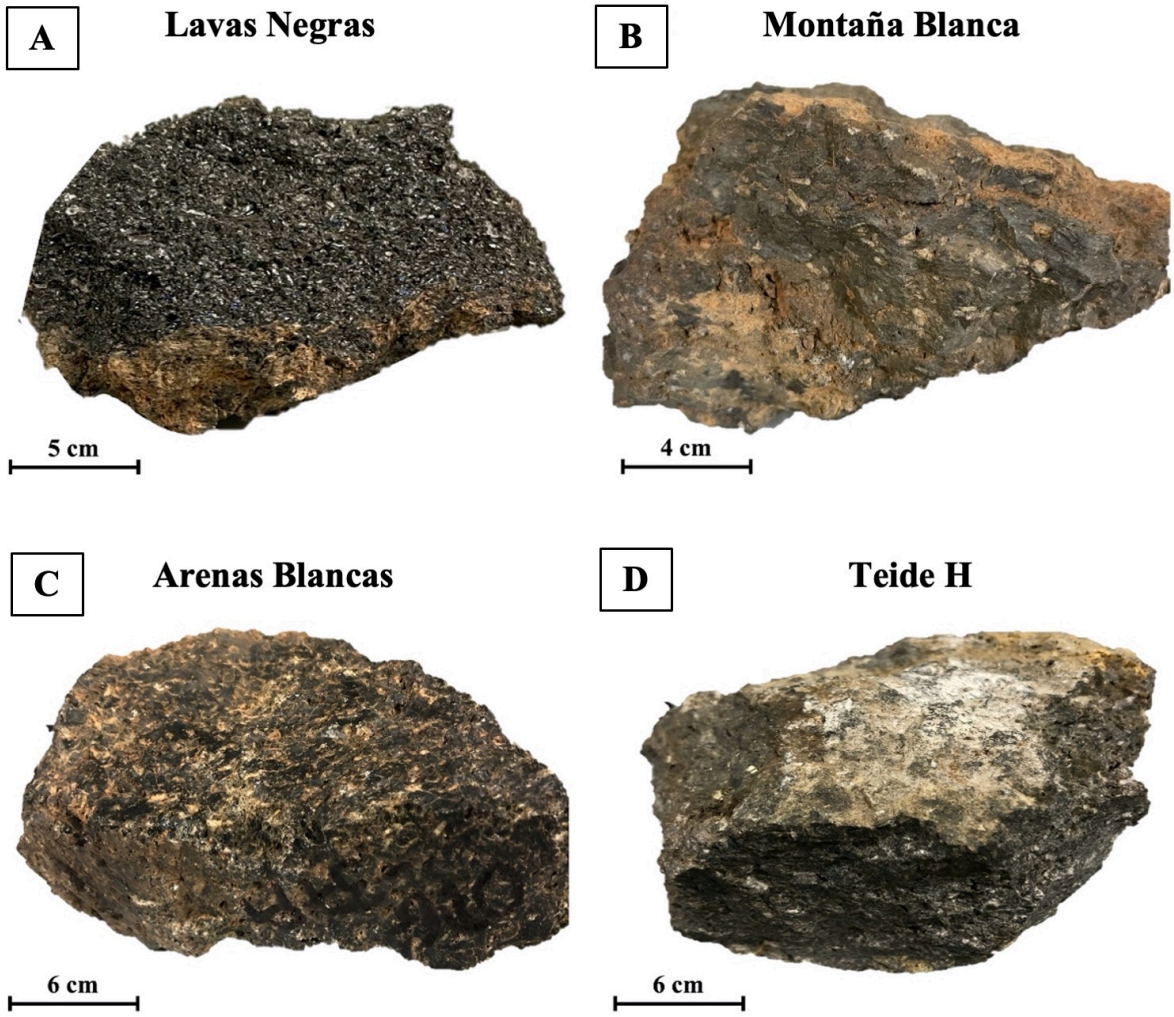

100

Figure DR2. Images of the alkali feldspar crystals and/or crystal fragments analyzed for (^{226}Ra)/(^{230}Th) ages. Alkali feldspar crystals for A) Lavas Negras, B) Montaña Blanca, and C) Arenas Blancas.

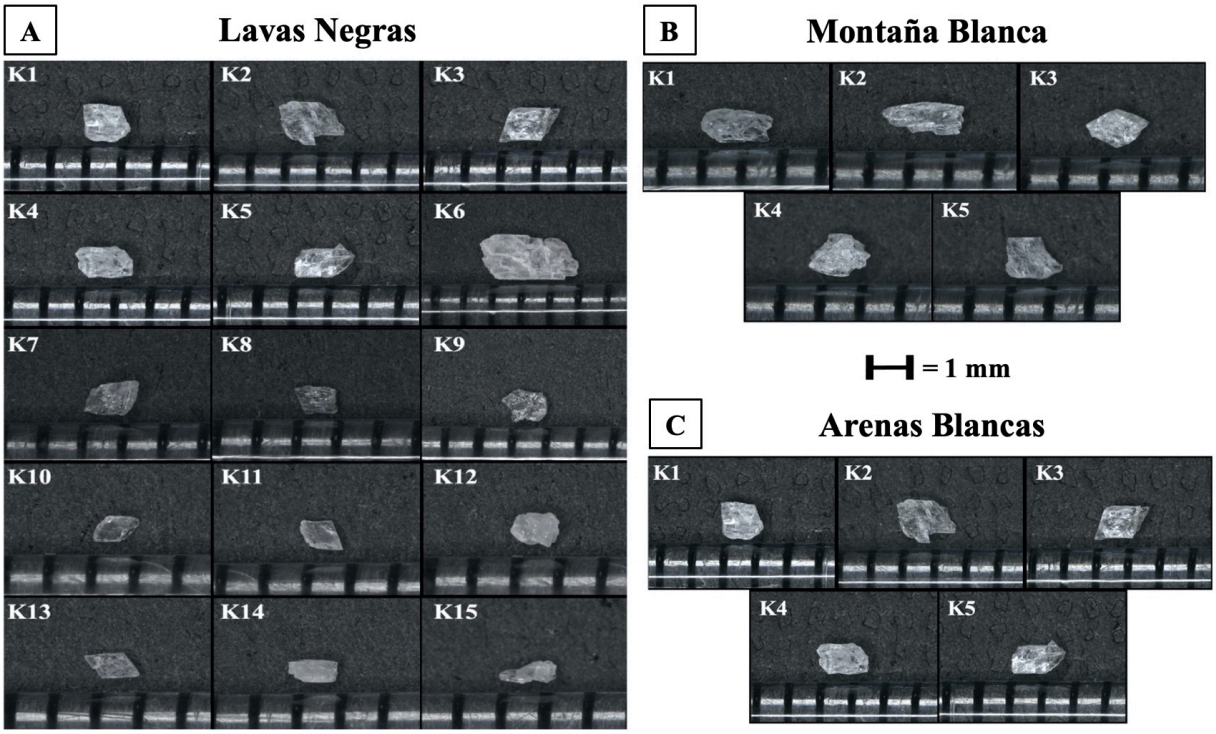

Figure DR3. Backscatter images of typical alkali feldspar crystals from A) Lavas Negras, B) Montaña Blanca, C) Arenas Blancas, and D) Teide H flows.

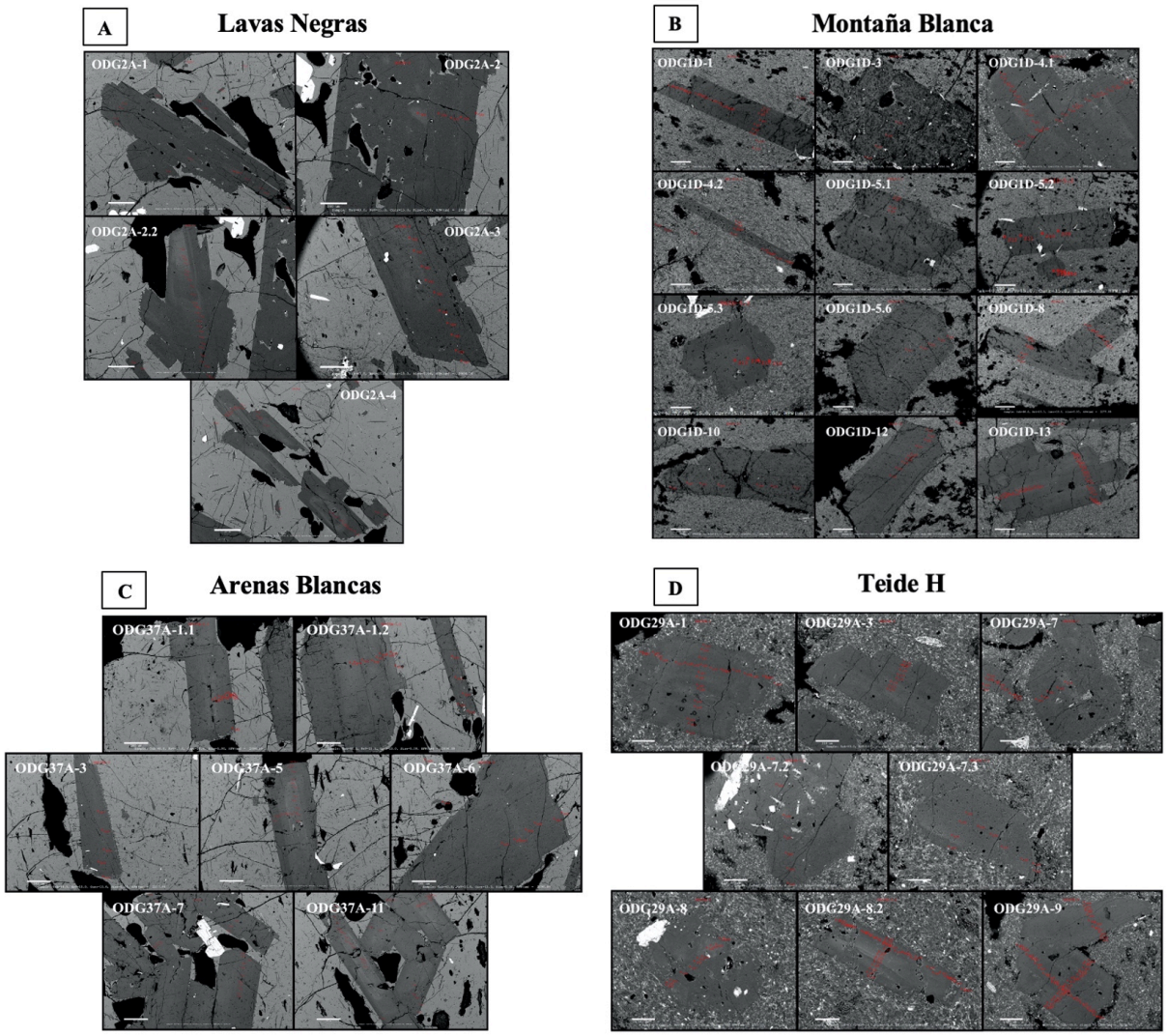

Figure DR4. Lattice Strain Model (LSM) curves used to determine D_{Ra}/D_{Ba} for single alkali feldspar crystals (K5, K10, K11, and K15) from the Lavas Negras flow.

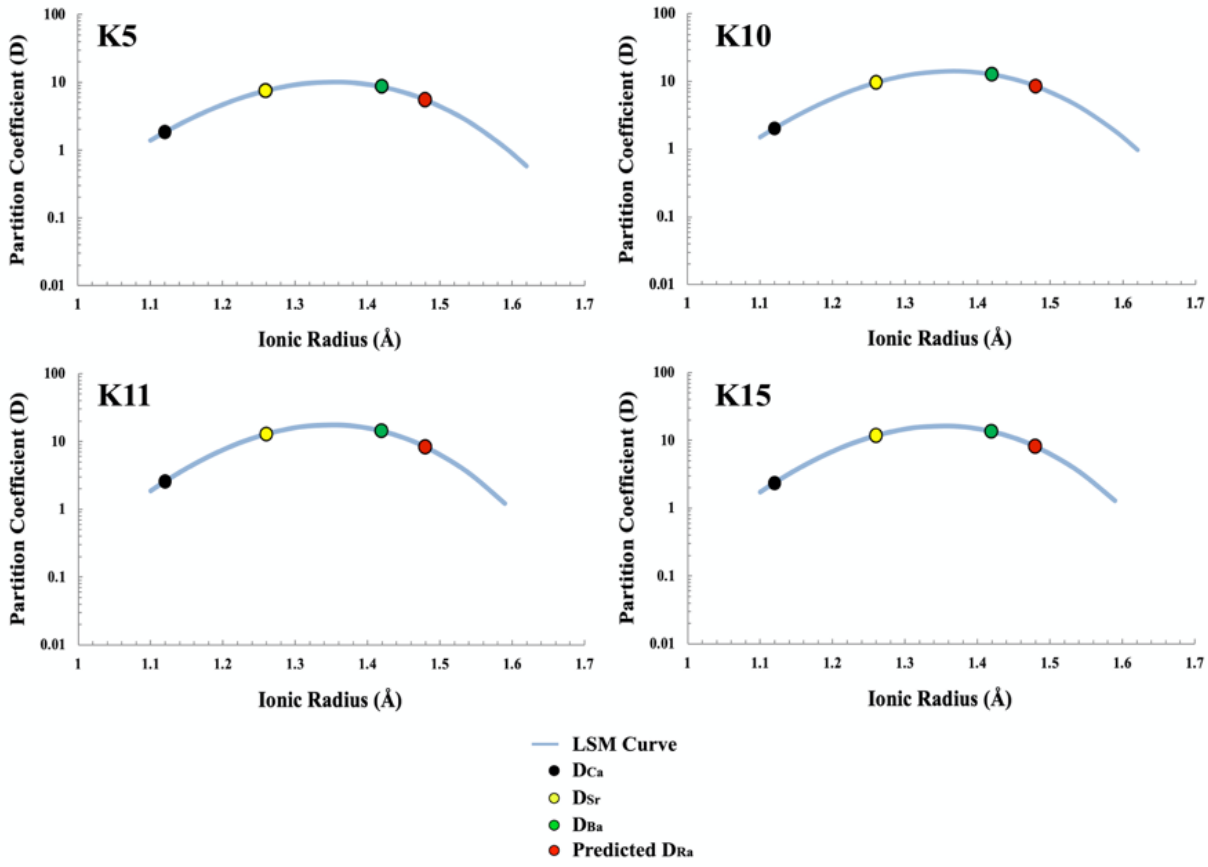

Figure DR5. Lattice Strain Model (LSM) curves used to determine D_{Ra}/D_{Ba} for the alkali feldspar separate (Xl. sep.) and single alkali feldspar crystals (K1, K2, K3 and K5) from the Montaña Blanca flow.

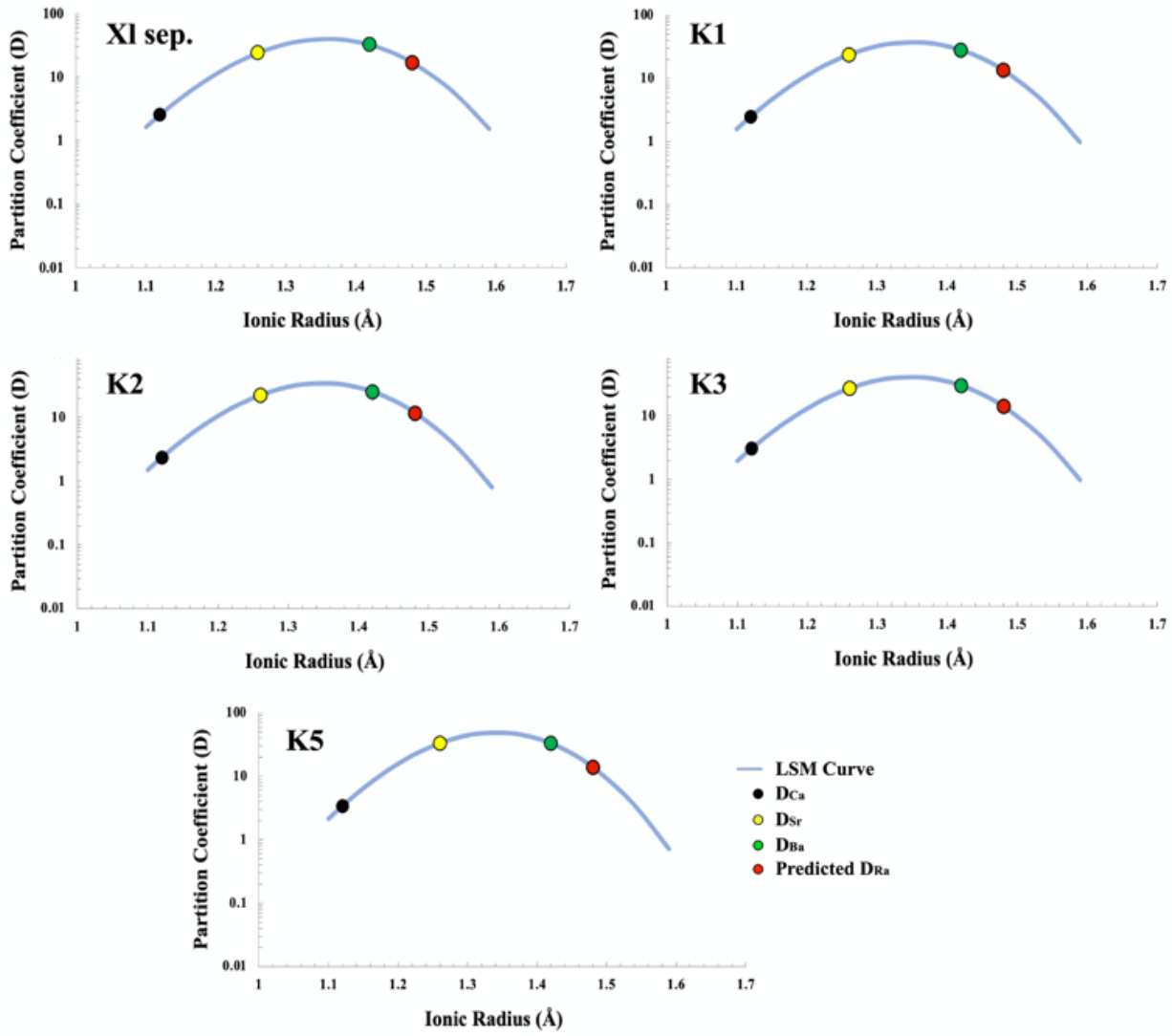

Figure DR6. Lattice Strain Model (LSM) curves used to determine D_{Ra}/D_{Ba} for the alkali feldspar separate (Xl. sep.) and single alkali feldspar crystals (K1–K5) from the Arenas Blancas flow.

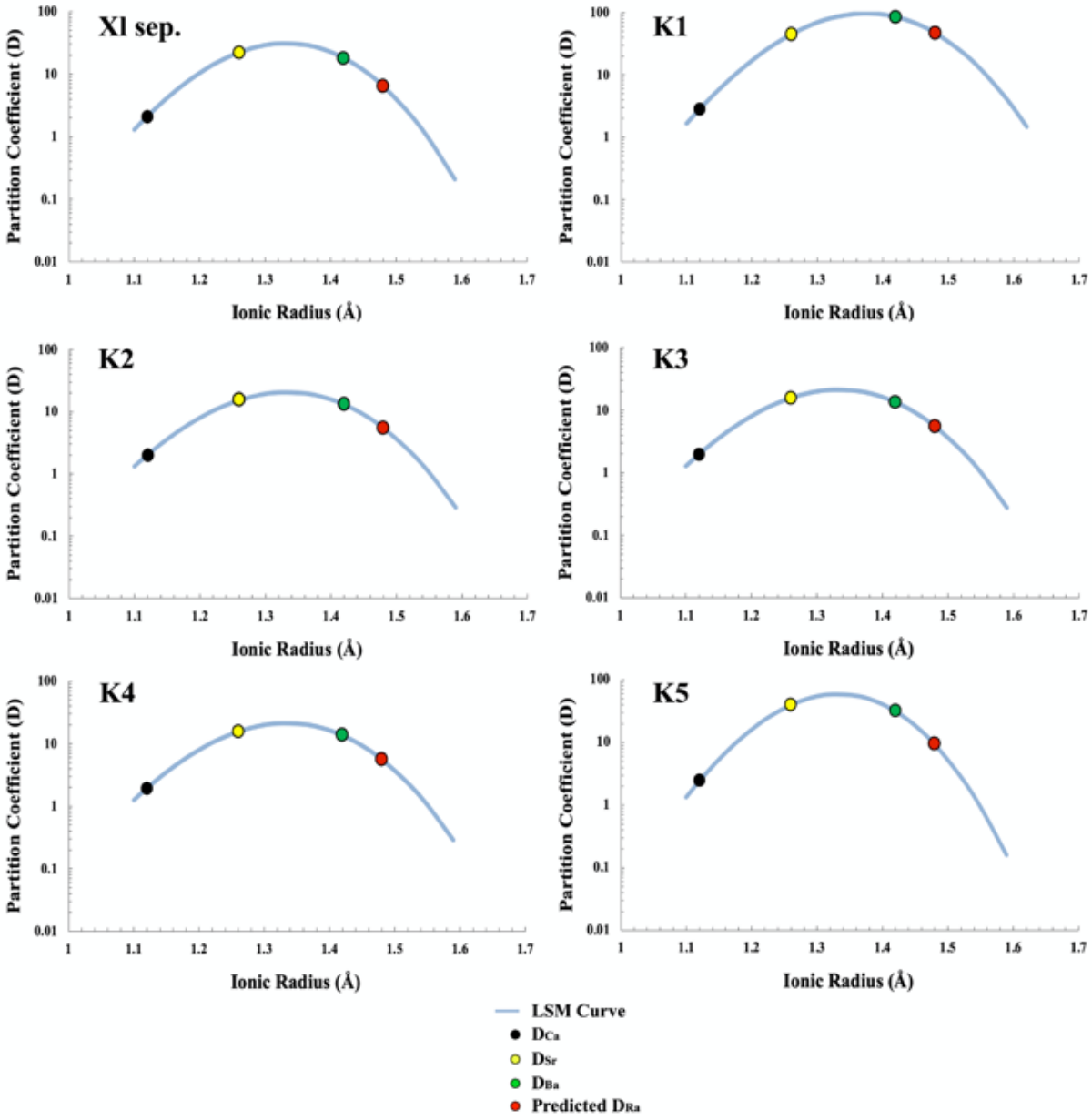

Figure DR7. Lattice Strain Model (LSM) curve used to determine D_{Ra}/D_{Ba} for the alkali feldspar separate from the Teide H flow.

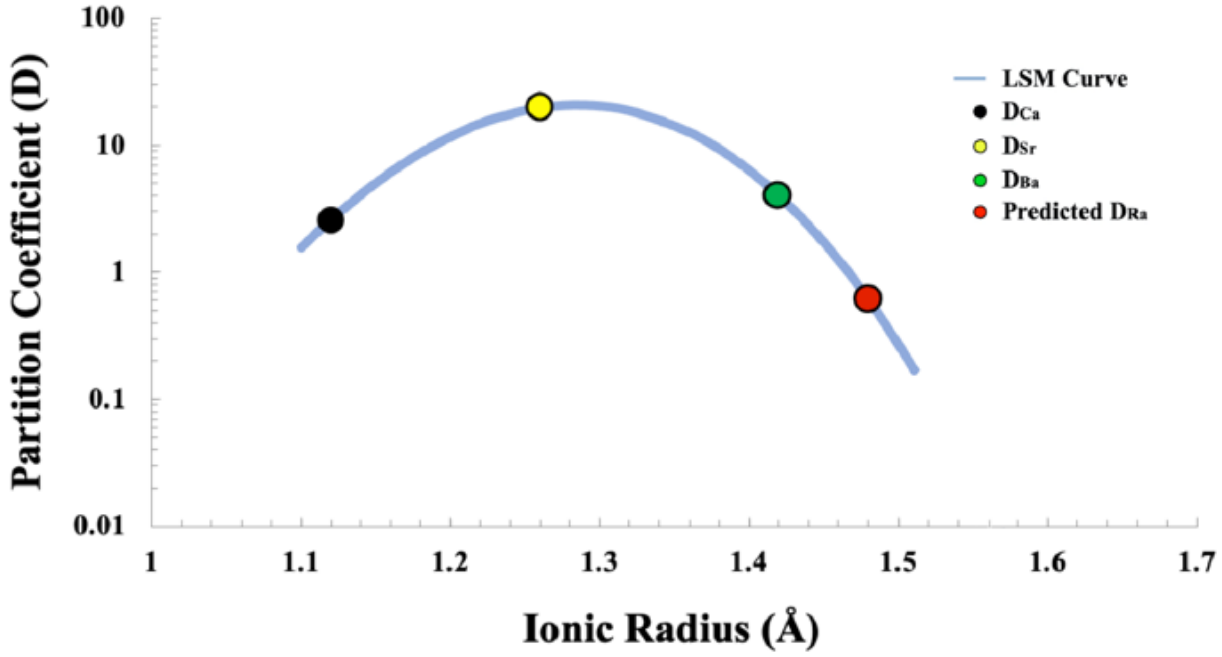

Figure DR8. Diagram showing ^{226}Ra concentration (fg/g) evolution of the melt (blue line) and feldspar (red line) through time for Lavas Negras K5. In general, the amount of ^{226}Ra in the crystal increases in the past, while the amount of ^{226}Ra in the melt decreases in the past. D_{Ra}/D_{Ba} are shown for crystal ages at the present (black), 400 a (green), 800 a (blue), and 1162 a (red), the target D_{Ra}/D_{Ba} for this feldspar.

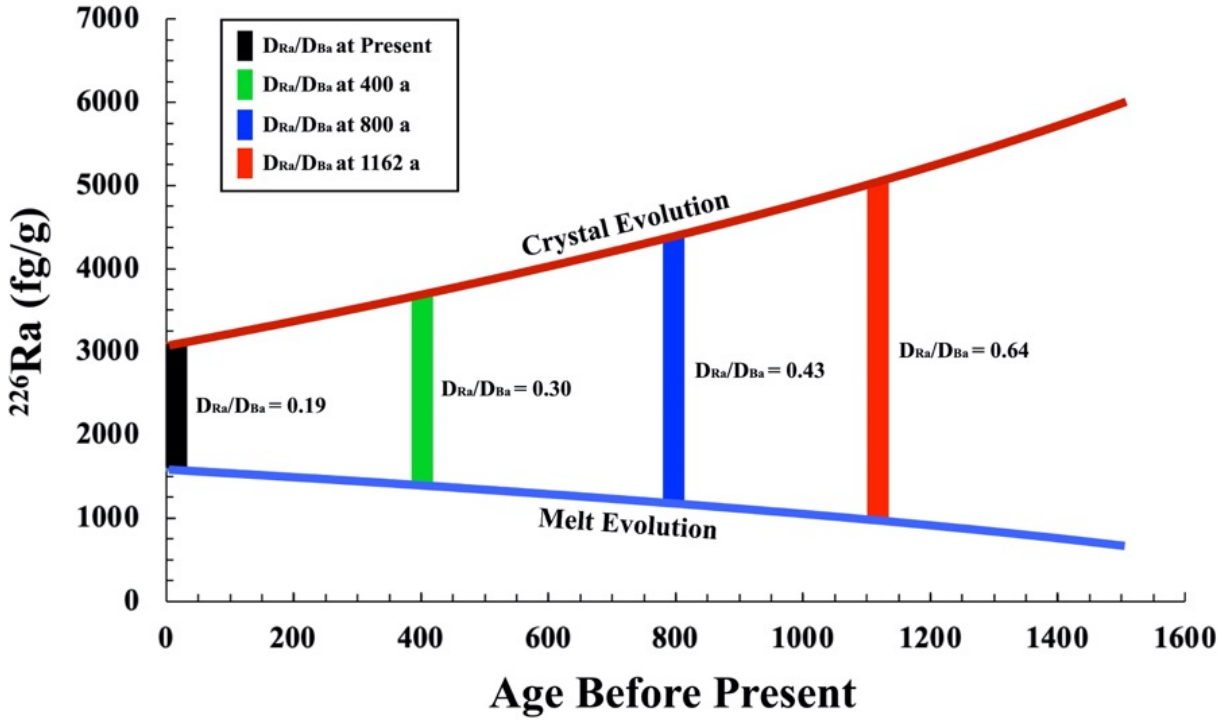

TABLE DR1. SUMMARY TABLE SHOWING CONCENTRATIONS OF ISOTOPE DILUTION DETERMINED CA, SR, AND BA IN SEQUENTIALLY DISSOLVED, CRYSTAL-FREE GROUNDMASS (GM), ALKALI FELDSPAR SEPARATES (XL. SEP.), AND INDIVIDUAL ALKALI FELDSPAR CRYSTALS (K).

Sample	Digestion	Ca (ppm)	Ba (ppm)	Sr (ppm)
Lavas Negras				
GM	Sequential	3,544	200	39
Xl. Sep.	Direct	8,337	4,142	265
K1	Direct	4,616	1,711	88
K2	Direct	8,801	3,453	161
K3	Direct	10,180	4,846	196
K4	Direct	7,974	2,083	124
K5	Direct	6,526	1,716	294
K6	Direct	8,834	2,322	109
K7	Direct	7,158	1,805	200
K8	Direct	10,678	3,501	152
K9	Direct	10,315	3,675	163
K10	Direct	7,179	2,519	374
K11	Direct	9,148	2,849	502
K12	Direct	7,337	2,586	148
K13	Direct	15,395	5,503	252
K14	Direct	7,125	1,126	276
K15	Direct	8,360	2,683	455
Montaña Blanca				
GM	Sequential	3,668	197	14
Xl. Sep.	Direct	9,317	6,331	335
K1	Direct	9,063	5,522	328
K2	Direct	8,662	5,010	312
K3	Direct	11,294	5,976	383
K4	Direct	3,417	7,187	445
K5	Direct	12,466	6,480	460
Arenas Blancas				
GM	Sequential	3,577	167	8
Xl. Sep.	Direct	7,558	3,023	177
K1	Direct	10,060	14,274	359
K2	Direct	7,217	2,194	123
K3	Direct	7,121	2,257	126
K4	Direct	6,992	2,297	126
K5	Direct	8,669	5,299	318
Teide H				
GM	Sequential	8,097	373	52
Xl. Sep.	Direct	21,026	1,506	1,033

Uncertainties associated with Ca, Ba, and Sr concentrations are <2%. The Ca/Ba and Rb/Sr spikes used to determine concentrations were calibrated to BCR-C, an analog of USGS BCR-1, with Ca = 6.98 wt %, Ba = 685 ppm, and Sr = 335 ppm.

TABLE DR2. SUMMARY TABLE SHOWING URANIUM, THORIUM, AND RADIUM CONCENTRATIONS OF SEQUENTIALLY DISSOLVED, CRYSTAL-FREE GROUNDMASS (GM), ALKALI FELDSPAR SEPARATES (XL. SEP.), INDIVIDUAL ALKALI FELDSPAR CRYSTALS (K), PERCENTAGE OF MELT INCLUSIONS, D_{Ra}/D_{Ba}, AND RA/TH DETERMINED CRYSTAL AGES.

Sample	U (ppm)	Th (ppm)	Ra (fg/g)	% MI	D_{Ra}/D_{Ba}	Crystal Age (a)
Lavas Negras						
GM	6.9	27.7	1,599			
Xl. Sep.	0.22	1.43	4,503	2.82%	N/D	N/D
K1	0.06	0.20	4,161	0.87%	N/D	N/D
K2	0.09	0.27	3,986	1.30%	N/D	N/D
K3	0.05	0.15	3,907	0.72%	N/D	N/D
K4	0.09	0.32	3,736	1.30%	N/D	N/D
K5	0.04	0.14	3,115	0.58%	0.64	1162 ± 116 a
K6	0.06	0.19	3,472	0.87%	N/D	N/D
K7	0.12	0.10	4,268	1.73%	N/D	N/D
K8	0.11	0.40	4,905	1.59%	N/D	N/D
K9	0.05	0.19	5,174	0.72%	N/D	N/D
K10	0.04	0.18	3,590	0.58%	0.67	1380 ± 138 a
K11	0.09	0.25	4,425	1.30%	0.59	1212 ± 121 a
K12	0.02	0.40	4,331	0.29%	N/D	N/D
K13	0.12	0.49	5,300	1.73%	N/D	N/D
K14	0.03	0.32	3,433	0.43%	N/D	N/D
K15	0.10	0.14	3,662	1.45%	0.60	1333 ± 133 a
Montaña Blanca						
GM	7.2	30.3	2,543			
Xl. Sep.	0.04	0.13	203	0.55%	0.53	5331 ± 533 a
K1	0.12	0.14	N/D	1.65%	N/D	N/D
K2	0.06	0.11	0	0.83%	0.47	>8000 a
K3	0.12	0.28	0	1.65%	0.47	>8000 a
K4	0.07	0.38	0	0.97%	N/D	N/D
K5	0.07	0.16	0	0.97%	0.43	>8000 a
Arenas Blancas						
GM	7.8	32.5	2,623			
Xl. Sep.	0.12	0.43	273	0.87%	0.36	4169 ± 417 a
K1	0.28	0.46	0	3.60%	0.55	>8000 a
K2	0.12	0.85	516	1.54%	0.42	3937 ± 394 a
K3	0.07	0.95	377	0.90%	0.41	4052 ± 405 a
K4	0.04	0.38	384	0.51%	0.41	4053 ± 405 a
K5	0.09	0.19	146	1.16%	0.30	>8000 a
Teide H						
GM	7.2	28.5	2,477			
Xl. Sep.	0.08	0.29	25	1.11%	0.15	>8000 a

U, Th, and Ra concentrations have errors of ≤2%. Alkali feldspar Ra concentrations have been corrected for the presence of melt inclusions, assuming that melt inclusions have the same Ra concentrations as the host melt, as reflected by the crystal-free groundmass (GM). D_{Ra}/D_{Ba} ratios have errors estimated at ~10%, which largely arise from errors associated with individual partition coefficients of Ca, Sr, and Ba. Errors associated with D_{Ca}, D_{Sr}, and D_{Ba} used for Onuma curve calculations are 2%, 0.3%, and 0.3% respectively.

TABLE DR3. SUMMARY TABLE SHOWING RADIOGENIC ISOTOPE RATIOS OF SEQUENTIALLY DISSOLVED, CRYSTAL-FREE GROUNDMASS (GM), ALKALI FELDSPAR SEPARATES (XL. SEP.), AND INDIVIDUAL ALKALI FELDSPAR CRYSTALS (K).

Sample*	$^{87}Sr/^{86}Sr$	$^{143}Nd/^{144}Nd$	$^{206}Pb/^{204}Pb$	$^{207}Pb/^{204}Pb$	$^{208}Pb/^{204}Pb$
Lavas Negras					
GM	0.703229 ± 0.000011	0.512875 ± 0.000004	19.756 ± 0.001	15.603 ± 0.001	39.534 ± 0.002
Xl. Sep.	0.703132 ± 0.000011		19.765 ± 0.002	15.599 ± 0.002	39.543 ± 0.002
K1	0.703140 ± 0.000010		19.772 ± 0.003	15.608 ± 0.002	39.578 ± 0.006
K2	0.703170 ± 0.000016		19.849 ± 0.010	15.666 ± 0.008	39.752 ± 0.022
K3	0.703226 ± 0.000013		19.751 ± 0.012	15.591 ± 0.010	39.552 ± 0.018
K4	0.703191 ± 0.000030		19.728 ± 0.008	15.615 ± 0.006	39.558 ± 0.016
K5	0.703225 ± 0.000011		19.640 ± 0.010	15.616 ± 0.008	39.459 ± 0.014
K6	0.703117 ± 0.000017		19.379 ± 0.010	15.592 ± 0.008	39.119 ± 0.016
*K7	0.703124 ± 0.000015		19.692 ± 0.004	15.584 ± 0.004	39.448 ± 0.008
*K8	0.703147 ± 0.000017		19.587 ± 0.028	15.652 ± 0.028	39.698 ± 0.040
*K9	0.703111 ± 0.000011		19.472 ± 0.024	15.621 ± 0.018	39.503 ± 0.018
*K10	0.703140 ± 0.000010		19.608 ± 0.022	15.627 ± 0.020	39.663 ± 0.030
*K11	0.703160 ± 0.000013		19.408 ± 0.028	15.538 ± 0.024	39.430 ± 0.036
*K12	0.703161± 0.000015		19.719 ± 0.018	15.628 ± 0.014	39.652 ± 0.024
*K13	0.703250 ± 0.000018		19.521 ± 0.036	15.730 ± 0.030	39.900 ± 0.042
*K14	N/A		19.695 ± 0.022	15.645 ± 0.020	39.687 ± 0.032
*K15	0.703184 ± 0.000014		19.657 ± 0.016	15.566 ± 0.014	39.447 ± 0.024
Montaña Blanca					
GM	0.704770 ± 0.000008	0.512870 ± 0.000005	19.739 ± 0.001	15.603 ± 0.001	39.523 ± 0.002
Xl. Sep.	0.703135 ± 0.000007		19.739 ± 0.005	15.583 ± 0.002	39.490 ± 0.001
K1	0.703126 ± 0.000010		19.653 ± 0.016	15.624 ± 0.014	39.446 ± 0.024
K2	0.703120 ± 0.000011		19.651 ± 0.016	15.542 ± 0.012	39.406 ± 0.028
K3	0.703128 ± 0.000012		19.605 ± 0.020	15.647 ± 0.016	39.488 ± 0.032
K4	0.703107 ± 0.000008		19.734 ± 0.018	15.609 ± 0.014	39.564 ± 0.030
K5	0.703147 ± 0.000012		19.436 ± 0.018	15.616 ± 0.016	39.277 ± 0.030
Arenas Blancas					
GM	0.703501 ± 0.000010	0.512876 ± 0.000004	19.756 ± 0.001	15.605 ± 0.001	39.543 ± 0.002
Xl. Sep.	0.703153 ± 0.000010		19.754 ± 0.001	15.607 ± 0.001	39.533 ± 0.002
K1	0.703150 ± 0.000011		19.719 ± 0.016	15.581 ± 0.012	39.502 ± 0.040
K2	0.703115 ± 0.000038		19.757 ± 0.010	15.605 ± 0.008	39.586 ± 0.024
K3	0.703086 ± 0.000021		19.756 ± 0.012	15.610 ± 0.010	39.576 ± 0.020
K4	0.703109 ± 0.000011		19.751 ± 0.014	15.598 ± 0.010	39.555 ± 0.026
K5	0.703136 ± 0.000008		19.762 ± 0.022	15.867 ± 0.008	39.602 ± 0.048
Teide H					
GM	0.703335 ± 0.000008	0.512880 ± 0.000004	19.751 ± 0.004	15.600 ± 0.002	39.516 ± 0.002
Xl. Sep.	0.703174 ± 0.000022		19.670 ± 0.042	15.602 ± 0.018	39.473 ± 0.058

* Lavas Negras crystals K7–K15 were affected by Pb blank resulting from small crystal sizes. Therefore, $^{206}Pb/^{204}Pb$, $^{207}Pb/^{204}Pb$, and $^{208}Pb/^{204}Pb$ are considered inaccurate (and not blank corrected).

Sr isotope ratios were determined using TIMS, and Pb and Nd isotope ratios were determined using MC-ICP-MS. NBS987 Sr standard during the analytical period for groundmass and feldspars was $^{87}Sr/^{86}Sr$: 0.710275 ± 0.000040 (n = 14). JNdi-1 Nd standard was $^{143}Nd/^{144}Nd$: 0.512091 ± 0.000004 (n = 6). NBS981 Pb standard (n = 16) was $^{206}Pb/^{204}Pb$: 16.929 ± 0.003, $^{207}Pb/^{204}Pb$: 15.481 ± 0.003, and $^{208}Pb/^{204}Pb$: 36.667 ± 0.002. Uncertainties for all analyses are 2σ.

TABLE DR4. SUMMARY TABLE SHOWING U-SERIES ACTIVITY RATIOS OF SEQUENTIALLY DISSOLVED, CRYSTAL-FREE GROUNDMASS (GM).

Sample	$(^{230}Th)/(^{232}Th)$	$(^{238}U)/(^{232}Th)$	$(^{230}Th)/(^{238}U)$	$(^{226}Ra)/(^{230}Th)$
Lavas Negras				
GM	0.866 ± 0.003	0.790 ± 0.008	1.096 ± 0.05	0.622 ± 0.02
Montaña Blanca				
GM	0.868 ± 0.002	0.761 ± 0.008	1.140 ± 0.05	0.914 ± 0.02
Arenas Blancas				
GM	0.867 ± 0.003	0.728 ± 0.008	1.191 ± 0.05	0.876 ± 0.02
Teide H				
GM	0.852 ± 0.003	0.768 ± 0.008	1.109 ± 0.05	0.925 ± 0.02

An uncertainty of ~1% is estimated for $(^{230}Th)/(^{232}Th)$ based on replicate analyses of BCR-C, TML, and AGV1 rock references. An uncertainty of ≤2% for $(^{238}U)/(^{232}Th)$ and $(^{226}Ra)/(^{230}Th)$ is estimated based on replicate analyses of BCR-C. $(^{230}Th)/(^{238}U)$ describes the degree of Th enrichment for each sample (e.g., 9.6% for Lavas Negras). Reference samples of TML were used to calibrate U/Th and Ra spikes and samples of BCR-C were used to evaluate the accuracy and reproducibility of U/Th and Ra/Th ratios. TML (n = 3) had an average $(^{226}Ra)/(^{230}Th)$ and $(^{230}Th)/(^{238}U)$ of 1.006 and 1.088, respectively, over the analytical period. BCR-C (n = 2) had an average $(^{226}Ra)/(^{230}Th)$ and $(^{230}Th)/(^{238}U)$ of 0.986 and 0.877, respectively, over the analytical period. U, Th, and Ra decay constants used were $\lambda_{238} = 1.55135 \times 10^{-10}$, $\lambda_{232} = 4.93343 \times 10^{-11}$, $\lambda_{230} = 9.21738 \times 10^{-6}$, and $\lambda_{226} = 4.3322 \times 10^{-4}$. BCR-C is a Columbia River basalt, powdered using a tungsten carbide shatterbox, collected from the same sampling site as USGS BCR-1 standard.

TABLE DR5. SUMMARY TABLE SHOWING PERCENTAGES OF ORTHOCLASE (Or), ALBITE (Ab), AND ANORTHITE (An) CONTENTS FOR LAVAS NEGRAS, MONTAÑA BLANCA, ARENAS BLANCAS, AND TEIDE H FELDSPARS.

Eruption	Sample	Distance from Core (µm)	%Or	%Ab	%An
Lavas Negras	ODG2A-1	0.0	24.23	69.02	6.76
Lavas Negras	ODG2A-1	30.1	26.38	68.60	5.02
Lavas Negras	ODG2A-1	76.4	26.46	67.80	5.74
Lavas Negras	ODG2A-1	191.8	29.11	67.02	3.88
Lavas Negras	ODG2A-1	386.0	26.20	68.61	5.20
Lavas Negras	ODG2A-1	471.5	26.12	68.40	5.47
Lavas Negras	ODG2A-1	780.7	27.41	67.75	4.84
Lavas Negras	ODG2A-1	3056.9	24.58	68.56	6.86
Lavas Negras	ODG2A-1	3121.4	25.18	68.86	5.96
Lavas Negras	ODG2A-1	3258.0	23.29	69.58	7.13
Lavas Negras	ODG2A-1	3323.4	22.78	69.40	7.82
Lavas Negras	ODG2A-1	3902.7	25.43	69.22	5.34
Lavas Negras	ODG2A-1	4478.8	28.11	67.42	4.46
Lavas Negras	ODG2A-1	4593.8	26.97	67.55	5.48
Lavas Negras	ODG2A-1	4892.0	19.25	70.64	10.11
Lavas Negras	ODG2A-1	6532.2	28.11	66.55	5.34
Lavas Negras	ODG2A-1	6829.3	26.94	68.39	4.67
Lavas Negras	ODG2A-2	0.0	28.73	66.40	4.87
Lavas Negras	ODG2A-2	204.7	28.39	67.42	4.19
Lavas Negras	ODG2A-2	333.5	29.49	66.75	3.76
Lavas Negras	ODG2A-2	429.0	20.99	70.41	8.61
Lavas Negras	ODG2A-2.2	0.0	27.12	67.24	5.64
Lavas Negras	ODG2A-2.2	76.3	25.90	67.83	6.27
Lavas Negras	ODG2A-2.2	112.1	25.60	68.27	6.13
Lavas Negras	ODG2A-2.2	158.8	24.59	68.49	6.92
Lavas Negras	ODG2A-2.2	239.0	24.36	68.81	6.83
Lavas Negras	ODG2A-2.2	276.3	25.29	68.73	5.98
Lavas Negras	ODG2A-2.2	338.8	25.72	68.35	5.94
Lavas Negras	ODG2A-2.2	415.3	25.33	69.19	5.49
Lavas Negras	ODG2A-2.2	501.8	25.62	69.13	5.25
Lavas Negras	ODG2A-2.2	591.6	26.44	68.95	4.61
Lavas Negras	ODG2A-2.2	632.8	24.79	68.99	6.22
Lavas Negras	ODG2A-2.2	666.9	23.98	68.91	7.11
Lavas Negras	ODG2A-2.2	718.4	24.18	68.88	6.94
Lavas Negras	ODG2A-2.2	779.1	23.59	69.71	6.70
Lavas Negras	ODG2A-2.2	833.5	24.11	69.42	6.47
Lavas Negras	ODG2A-2.2	888.6	24.83	68.84	6.33
Lavas Negras	ODG2A-2.2	944.8	25.16	68.96	5.88
Lavas Negras	ODG2A-2.2	1008.1	26.73	68.09	5.18
Lavas Negras	ODG2A-2.2	1076.3	28.17	67.34	4.49
Lavas Negras	ODG2A-2.2	1122.8	24.80	69.49	5.71
Lavas Negras	ODG2A-2.2	1205.3	25.65	68.84	5.51
Lavas Negras	ODG2A-2.2	1271.5	25.75	68.58	5.67
Lavas Negras	ODG2A-2.2	1345.7	25.90	68.50	5.61
Lavas Negras	ODG2A-2.2	1441.8	25.14	69.29	5.57
Lavas Negras	ODG2A-2.2	1479.8	26.23	68.21	5.55
Lavas Negras	ODG2A-2.2	1543.7	17.02	72.56	10.43
Lavas Negras	ODG2A-2.2	2451.0	24.18	69.18	6.63
Lavas Negras	ODG2A-3	0.0	26.67	67.86	5.47
Lavas Negras	ODG2A-3	197.0	29.87	66.54	3.59
Lavas Negras	ODG2A-3	450.7	30.52	65.84	3.64
Lavas Negras	ODG2A-3	659.8	28.82	67.07	4.11
Lavas Negras	ODG2A-3	874.7	30.00	66.35	3.65
Lavas Negras	ODG2A-3	1148.9	30.31	66.43	3.26
Lavas Negras	ODG2A-3	1364.5	30.15	66.27	3.59
Lavas Negras	ODG2A-3	1543.1	26.89	68.17	4.94
Lavas Negras	ODG2A-3	1779.7	29.58	66.78	3.64
Lavas Negras	ODG2A-3	1949.9	25.71	68.89	5.40
Lavas Negras	ODG2A-4	0.0	15.76	71.65	12.59
Lavas Negras	ODG2A-4	28.1	24.00	69.54	6.46
Lavas Negras	ODG2A-4	51.3	22.88	69.39	7.73
Lavas Negras	ODG2A-4	86.4	26.08	67.84	6.08
Lavas Negras	ODG2A-4	112.9	26.34	68.39	5.27
Lavas Negras	ODG2A-4	133.2	25.83	68.24	5.93
Lavas Negras	ODG2A-4	181.9	24.68	68.44	6.87
Lavas Negras	ODG2A-4	214.5	26.39	68.49	5.12
Lavas Negras	ODG2A-4	516.1	23.00	69.44	7.56
Lavas Negras	ODG2A-4	604.9	25.99	69.44	4.57
Lavas Negras	ODG2A-4	631.1	24.78	69.02	6.20
Lavas Negras	ODG2A-4	673.2	23.23	69.26	7.51
Lavas Negras	ODG2A-4	1886.3	27.67	67.59	4.74

Lavas Negras	ODG2A-4	1937.6	27.84	67.74	4.42
Lavas Negras	ODG2A-4	2009.3	25.74	68.10	6.16
Lavas Negras	ODG2A-4	2054.0	21.75	69.74	8.51
Lavas Negras	ODG2A-4	2083.0	21.05	70.19	8.76
Lavas Negras	ODG2A-4	2115.6	27.15	68.42	4.43
Lavas Negras	ODG2A-4	2164.1	26.19	68.17	5.64
Lavas Negras	ODG2A-4	2219.9	24.61	69.27	6.13
Lavas Negras	ODG2A-4	2512.6	25.59	69.02	5.39
Lavas Negras	ODG2A-4	2599.2	25.50	68.80	5.70
Lavas Negras	ODG2A-4	3652.5	25.51	68.65	5.83
Lavas Negras	ODG2A-4	6127.1	25.19	69.26	5.55
Montaña Blanca	ODG1D-3	0.0	22.45	70.53	7.02
Montaña Blanca	ODG1D-3	256.6	21.42	69.54	9.03
Montaña Blanca	ODG1D-3	486.8	21.36	70.44	8.19
Montaña Blanca	ODG1D-3	720.7	25.07	67.87	7.06
Montaña Blanca	ODG1D-5.1	0.0	26.82	67.72	5.45
Montaña Blanca	ODG1D-5.1	49.9	23.91	69.36	6.74
Montaña Blanca	ODG1D-5.1	177.4	28.88	66.93	4.20
Montaña Blanca	ODG1D-5.2	0.0	28.98	66.63	4.39
Montaña Blanca	ODG1D-5.2	304.5	31.04	65.69	3.28
Montaña Blanca	ODG1D-5.2	1019.0	27.29	67.58	5.12
Montaña Blanca	ODG1D-5.3	0.0	24.75	69.37	5.88
Montaña Blanca	ODG1D-5.3	76.3	24.27	69.24	6.49
Montaña Blanca	ODG1D-5.3	136.6	25.80	69.53	4.66
Montaña Blanca	ODG1D-5.3	202.7	25.75	67.91	6.35
Montaña Blanca	ODG1D-5.6	0.0	22.64	69.83	7.53
Montaña Blanca	ODG1D-5.6	166.0	24.25	68.87	6.88
Montaña Blanca	ODG1D-5.6	260.9	22.45	69.97	7.58
Montaña Blanca	ODG1D-5.6	381.7	25.74	68.43	5.83
Montaña Blanca	ODG1D-5.6	483.5	32.52	63.79	3.69
Montaña Blanca	ODG1D-10	0.0	25.49	69.76	4.75
Montaña Blanca	ODG1D-10	293.6	25.93	68.86	5.22
Montaña Blanca	ODG1D-10	476.3	25.47	69.99	4.54
Montaña Blanca	ODG1D-10	973.7	30.90	65.97	3.14
Montaña Blanca	ODG1D-10	1210.6	31.66	65.33	3.00
Montaña Blanca	ODG1D-10	1381.3	30.64	66.02	3.33
Montaña Blanca	ODG1D-10	1602.6	31.48	65.31	3.20
Montaña Blanca	ODG1D-12	0.0	28.32	67.41	4.27
Montaña Blanca	ODG1D-12	124.6	28.03	67.92	4.06
Montaña Blanca	ODG1D-12	232.9	27.61	68.06	4.33
Montaña Blanca	ODG1D-12	295.3	27.82	67.94	4.24
Montaña Blanca	ODG1D-12	344.5	27.26	67.79	4.95
Montaña Blanca	ODG1D-12	392.1	26.98	68.56	4.46
Montaña Blanca	ODG1D-12	514.4	27.06	68.13	4.81
Montaña Blanca	ODG1D-12	651.5	27.34	68.28	4.38
Montaña Blanca	ODG1D-12	722.5	28.44	67.47	4.09
Montaña Blanca	ODG1D-12	803.5	26.75	68.27	4.98
Montaña Blanca	ODG1D-1	0.0	25.57	67.98	6.46
Montaña Blanca	ODG1D-1	57.2	27.48	68.25	4.26
Montaña Blanca	ODG1D-1	127.6	28.51	67.43	4.06
Montaña Blanca	ODG1D-1	222.5	27.87	67.41	4.73
Montaña Blanca	ODG1D-1	315.4	28.31	67.37	4.32
Montaña Blanca	ODG1D-1	372.5	27.79	67.67	4.54
Montaña Blanca	ODG1D-1	420.6	26.83	67.98	5.19
Montaña Blanca	ODG1D-1	1794.5	26.24	67.08	6.68
Montaña Blanca	ODG1D-1	1858.1	32.45	64.21	3.35
Montaña Blanca	ODG1D-1	1917.0	31.94	65.00	3.06
Montaña Blanca	ODG1D-1	1978.2	30.15	65.97	3.88
Montaña Blanca	ODG1D-1	2029.9	32.02	64.78	3.20
Montaña Blanca	ODG1D-1	2055.3	31.58	65.10	3.31
Montaña Blanca	ODG1D-1	2189.7	26.21	69.06	4.73
Montaña Blanca	ODG1D-1	2246.5	26.63	68.37	5.00
Montaña Blanca	ODG1D-1	2298.7	26.75	68.46	4.79
Montaña Blanca	ODG1D-1	2423.7	29.61	66.36	4.03
Montaña Blanca	ODG1D-1	2504.5	28.13	67.69	4.18
Montaña Blanca	ODG1D-1	2587.5	28.32	67.48	4.20
Montaña Blanca	ODG1D-1	2671.9	28.40	67.21	4.39
Montaña Blanca	ODG1D-1	2703.4	28.53	67.51	3.96
Montaña Blanca	ODG1D-8	58.8	27.52	67.31	5.17
Montaña Blanca	ODG1D-8	121.5	27.64	67.96	4.39
Montaña Blanca	ODG1D-8	244.9	28.04	67.42	4.54
Montaña Blanca	ODG1D-8	282.0	28.29	67.23	4.48
Montaña Blanca	ODG1D-8	363.5	27.37	67.72	4.91
Montaña Blanca	ODG1D-8	416.7	27.65	67.65	4.70
Montaña Blanca	ODG1D-8	1339.3	28.31	67.85	3.84
Montaña Blanca	ODG1D-8	1395.2	28.35	67.62	4.04
Montaña Blanca	ODG1D-8	1485.1	27.10	68.07	4.83
Montaña Blanca	ODG1D-8	1520.8	26.70	68.68	4.62
Montaña Blanca	ODG1D-8	1603.2	27.23	68.27	4.50
Montaña Blanca	ODG1D-8	1661.8	27.65	68.14	4.21

Montaña Blanca	ODG1D-13	0.0	24.37	69.51	6.12
Montaña Blanca	ODG1D-13	22.8	23.83	69.99	6.18
Montaña Blanca	ODG1D-13	52.2	23.01	70.08	6.91
Montaña Blanca	ODG1D-13	85.9	22.86	70.20	6.94
Montaña Blanca	ODG1D-13	140.4	22.73	69.66	7.61
Montaña Blanca	ODG1D-13	167.9	22.91	69.65	7.45
Montaña Blanca	ODG1D-13	219.2	23.58	69.23	7.20
Montaña Blanca	ODG1D-13	244.8	23.40	69.48	7.12
Montaña Blanca	ODG1D-13	298.4	22.65	70.67	6.68
Montaña Blanca	ODG1D-13	333.8	23.20	69.70	7.10
Montaña Blanca	ODG1D-13	372.9	22.11	70.33	7.56
Montaña Blanca	ODG1D-13	431.2	23.19	70.05	6.76
Montaña Blanca	ODG1D-13	475.0	23.35	69.90	6.75
Montaña Blanca	ODG1D-13	542.8	24.57	69.35	6.09
Montaña Blanca	ODG1D-13	591.2	26.06	68.75	5.18
Montaña Blanca	ODG1D-13	646.0	28.31	67.25	4.43
Montaña Blanca	ODG1D-13	717.6	30.47	66.16	3.38
Montaña Blanca	ODG1D-13	745.8	30.99	65.66	3.36
Montaña Blanca	ODG1D-13	780.2	29.05	67.04	3.91
Montaña Blanca	ODG1D-13	809.9	30.72	66.19	3.09
Montaña Blanca	ODG1D-13	1648.6	21.85	70.55	7.60
Montaña Blanca	ODG1D-13	1698.6	21.97	70.06	7.97
Montaña Blanca	ODG1D-13	1772.8	20.15	70.46	9.39
Montaña Blanca	ODG1D-13	1820.0	23.07	69.67	7.26
Montaña Blanca	ODG1D-13	1870.4	20.26	69.68	10.06
Montaña Blanca	ODG1D-13	1909.5	26.81	67.84	5.35
Montaña Blanca	ODG1D-13	1960.9	23.25	69.85	6.89
Montaña Blanca	ODG1D-13	2017.0	26.68	68.18	5.14
Montaña Blanca	ODG1D-13	2086.9	28.06	67.65	4.29
Montaña Blanca	ODG1D-13	2129.2	28.20	67.59	4.22
Montaña Blanca	ODG1D-13	2167.4	30.41	66.26	3.32
Montaña Blanca	ODG1D-13	2200.1	30.04	66.75	3.21
Montaña Blanca	ODG-1D-4.1	0.0	23.87	68.56	7.57
Montaña Blanca	ODG-1D-4.1	68.2	25.23	68.20	6.57
Montaña Blanca	ODG-1D-4.1	147.7	23.46	69.42	7.12
Montaña Blanca	ODG-1D-4.1	182.7	23.85	69.31	6.84
Montaña Blanca	ODG-1D-4.1	255.4	24.61	68.72	6.67
Montaña Blanca	ODG-1D-4.1	331.7	23.89	69.78	6.33
Montaña Blanca	ODG-1D-4.1	361.9	23.81	70.01	6.18
Montaña Blanca	ODG-1D-4.1	415.7	24.68	69.45	5.87
Montaña Blanca	ODG-1D-4.2	0.0	26.66	67.44	5.90
Montaña Blanca	ODG-1D-4.2	25.4	22.95	70.49	6.57
Montaña Blanca	ODG-1D-4.2	42.4	23.38	69.99	6.63
Montaña Blanca	ODG-1D-4.2	249.8	25.14	69.44	5.42
Montaña Blanca	ODG-1D-4.2	278.9	23.93	70.44	5.64
Montaña Blanca	ODG-1D-4.2	288.0	22.92	70.89	6.18
Montaña Blanca	ODG-1D-4.2	326.1	23.90	70.56	5.54
Montaña Blanca	ODG-1D-4.2	366.3	24.12	70.25	5.62
Montaña Blanca	ODG-1D-4.2	377.7	23.80	70.27	5.93
Montaña Blanca	ODG-1D-4.2	946.1	28.89	66.93	4.18
Montaña Blanca	ODG-1D-4.2	1181.9	23.89	67.39	8.73
Montaña Blanca	ODG-1D-4.2	1417.1	25.00	67.59	7.41
Arenas Blancas	ODG37A-1.1	0.0	21.51	70.30	8.18
Arenas Blancas	ODG37A-1.1	34.6	20.85	70.06	9.09
Arenas Blancas	ODG37A-1.1	78.5	20.56	70.32	9.11
Arenas Blancas	ODG37A-1.1	112.3	21.35	70.89	7.77
Arenas Blancas	ODG37A-1.1	147.5	21.66	70.94	7.39
Arenas Blancas	ODG37A-1.1	178.3	21.88	70.81	7.31
Arenas Blancas	ODG37A-1.1	204.5	22.64	70.47	6.88
Arenas Blancas	ODG37A-1.1	237.6	22.88	70.60	6.52
Arenas Blancas	ODG37A-1.1	261.4	22.13	70.72	7.16
Arenas Blancas	ODG37A-1.1	616.5	25.75	68.73	5.52
Arenas Blancas	ODG37A-1.2	0.0	22.98	69.82	7.20
Arenas Blancas	ODG37A-1.2	49.9	22.63	70.29	7.08
Arenas Blancas	ODG37A-1.2	133.6	22.26	70.67	7.06
Arenas Blancas	ODG37A-1.2	241.9	21.42	70.25	8.34
Arenas Blancas	ODG37A-1.2	306.9	22.49	70.02	7.49
Arenas Blancas	ODG37A-1.2	358.1	28.42	67.43	4.14
Arenas Blancas	ODG37A-1.2	436.8	22.56	69.56	7.87
Arenas Blancas	ODG37A-1.2	482.4	23.89	69.22	6.89
Arenas Blancas	ODG37A-1.2	1267.9	24.70	69.52	5.78
Arenas Blancas	ODG37A-1.2	1508.7	25.84	69.26	4.89
Arenas Blancas	ODG37A-1.2	1707.5	24.67	70.25	5.08
Arenas Blancas	ODG37A-1.2	1915.6	30.16	66.33	3.51
Arenas Blancas	ODG37A-1.2	2047.0	30.70	65.84	3.46
Arenas Blancas	ODG37A-3	0.0	31.57	65.46	2.98
Arenas Blancas	ODG37A-3	240.9	30.14	66.61	3.25
Arenas Blancas	ODG37A-3	481.9	29.66	66.54	3.80
Arenas Blancas	ODG37A-3	646.6	27.93	68.09	3.98
Arenas Blancas	ODG37A-3	837.0	27.59	68.08	4.33

Arenas Blancas	ODG37A-5	0.0	22.84	69.60	7.56
Arenas Blancas	ODG37A-5	78.4	22.27	69.87	7.86
Arenas Blancas	ODG37A-5	162.5	22.29	69.90	7.81
Arenas Blancas	ODG37A-5	263.2	22.52	69.58	7.90
Arenas Blancas	ODG37A-5	318.3	21.85	69.91	8.24
Arenas Blancas	ODG37A-5	434.9	21.72	70.39	7.89
Arenas Blancas	ODG37A-5	493.1	19.92	70.12	9.96
Arenas Blancas	ODG37A-5	538.4	26.92	68.40	4.69
Arenas Blancas	ODG37A-5	637.5	31.55	65.55	2.89
Arenas Blancas	ODG37A-5	710.7	27.84	67.58	4.58
Arenas Blancas	ODG37A-5	1338.0	22.36	69.64	8.01
Arenas Blancas	ODG37A-5	1391.8	26.34	68.27	5.39
Arenas Blancas	ODG37A-5	1450.9	23.20	69.91	6.90
Arenas Blancas	ODG37A-5	1472.1	22.92	70.11	6.97
Arenas Blancas	ODG37A-5	1527.2	24.93	69.08	5.99
Arenas Blancas	ODG37A-5	1569.6	26.82	68.92	4.26
Arenas Blancas	ODG37A-5	1601.1	27.13	68.04	4.83
Arenas Blancas	ODG37A-5	1655.1	28.36	67.61	4.03
Arenas Blancas	ODG37A-6	0.0	26.41	68.13	5.46
Arenas Blancas	ODG37A-6	142.6	26.06	68.55	5.39
Arenas Blancas	ODG37A-6	198.5	30.01	66.22	3.78
Arenas Blancas	ODG37A-6	328.5	28.29	67.53	4.18
Arenas Blancas	ODG37A-6	452.7	26.36	68.49	5.15
Arenas Blancas	ODG37A-6	665.0	29.86	66.71	3.43
Arenas Blancas	ODG37A-6	2074.0	27.91	67.45	4.64
Arenas Blancas	ODG37A-7	0.0	25.74	69.08	5.18
Arenas Blancas	ODG37A-7	34.1	26.55	67.87	5.58
Arenas Blancas	ODG37A-7	93.6	27.52	67.55	4.93
Arenas Blancas	ODG37A-7	141.2	27.67	67.24	5.09
Arenas Blancas	ODG37A-7	173.2	27.97	67.27	4.76
Arenas Blancas	ODG37A-7	247.7	26.59	68.35	5.06
Arenas Blancas	ODG37A-7	337.3	30.23	66.18	3.59
Arenas Blancas	ODG37A-7	387.6	29.83	66.23	3.94
Arenas Blancas	ODG37A-7	458.8	30.76	65.87	3.37
Arenas Blancas	ODG37A-7	541.6	31.96	65.19	2.85
Arenas Blancas	ODG37A-7	574.5	26.94	67.43	5.63
Arenas Blancas	ODG37A-7	950.7	29.22	66.85	3.93
Arenas Blancas	ODG37A-7	1043.6	26.89	68.61	4.50
Arenas Blancas	ODG37A-7	1101.7	28.81	67.22	3.97
Arenas Blancas	ODG37A-7	1855.1	26.70	67.76	5.54
Arenas Blancas	ODG37A-7	1894.3	26.81	68.29	4.90
Arenas Blancas	ODG37A-7	1936.2	26.45	69.15	4.40
Arenas Blancas	ODG37A-7	2353.1	26.16	68.49	5.34
Arenas Blancas	ODG37A-7	2467.4	25.32	69.36	5.32
Arenas Blancas	ODG37A-7	2568.2	25.75	69.64	4.61
Arenas Blancas	ODG37A-11	0.0	22.70	69.72	7.58
Arenas Blancas	ODG37A-11	49.3	23.38	70.04	6.58
Arenas Blancas	ODG37A-11	79.4	23.53	69.66	6.81
Arenas Blancas	ODG37A-11	108.1	23.47	69.81	6.72
Arenas Blancas	ODG37A-11	269.8	22.88	69.90	7.22
Arenas Blancas	ODG37A-11	312.5	23.04	69.23	7.73
Arenas Blancas	ODG37A-11	366.2	22.13	69.86	8.02
Arenas Blancas	ODG37A-11	414.5	23.28	69.18	7.54
Arenas Blancas	ODG37A-11	473.8	20.93	70.09	8.98
Arenas Blancas	ODG37A-11	508.6	31.32	65.58	3.11
Arenas Blancas	ODG37A-11	544.5	29.98	66.38	3.64
Arenas Blancas	ODG37A-11	616.4	28.80	67.22	3.99
Arenas Blancas	ODG37A-11	691.0	27.69	68.63	3.68
Arenas Blancas	ODG37A-11	763.1	29.61	66.43	3.97
Arenas Blancas	ODG37A-11	1708.2	22.19	70.06	7.75
Arenas Blancas	ODG37A-11	1728.4	22.72	70.12	7.16
Arenas Blancas	ODG37A-11	1768.0	25.25	69.05	5.69
Arenas Blancas	ODG37A-11	1790.7	24.97	69.34	5.68
Arenas Blancas	ODG37A-11	1858.4	26.96	68.16	4.88
Arenas Blancas	ODG37A-11	1902.6	27.44	67.73	4.83
Arenas Blancas	ODG37A-11	1936.3	28.16	67.60	4.23
Arenas Blancas	ODG37A-11	1971.8	29.52	66.61	3.87
Arenas Blancas	ODG37A-11	3058.7	22.83	69.96	7.21
Arenas Blancas	ODG37A-11	3166.1	23.35	70.91	5.74
Arenas Blancas	ODG37A-11	3216.7	31.04	65.98	2.98
Arenas Blancas	ODG37A-11	3309.0	29.91	66.15	3.94
Arenas Blancas	ODG37A-11	3401.6	31.84	64.66	3.49
Arenas Blancas	ODG37A-11	4426.9	22.98	69.65	7.37
Arenas Blancas	ODG37A-11	4540.8	24.66	69.09	6.25
Arenas Blancas	ODG37A-11	5595.1	25.26	70.03	4.71
Teide H	ODG29A-1	0.0	24.17	67.10	8.72
Teide H	ODG29A-1	62.3	24.28	66.94	8.78
Teide H	ODG29A-1	96.9	23.37	67.43	9.20
Teide H	ODG29A-1	198.6	21.66	67.99	10.35
Teide H	ODG29A-1	240.3	20.20	68.51	11.29

Teide H	ODG29A-1	330.7	17.77	69.37	12.86
Teide H	ODG29A-1	359.2	21.86	68.77	9.37
Teide H	ODG29A-1	417.8	20.50	67.13	12.37
Teide H	ODG29A-1	452.6	21.44	67.44	11.12
Teide H	ODG29A-1	509.8	22.25	67.91	9.84
Teide H	ODG29A-1	564.2	21.71	68.42	9.87
Teide H	ODG29A-1	623.7	22.55	66.60	10.84
Teide H	ODG29A-1	657.3	23.49	67.84	8.68
Teide H	ODG29A-1	1105.0	42.20	55.26	2.55
Teide H	ODG29A-1	1123.6	21.80	68.57	9.63
Teide H	ODG29A-1	1192.6	26.23	65.86	7.92
Teide H	ODG29A-1	1221.3	25.90	65.84	8.26
Teide H	ODG29A-1	1269.4	27.10	65.82	7.09
Teide H	ODG29A-1	1378.9	27.76	65.27	6.97
Teide H	ODG29A-1	1441.2	21.95	67.32	10.73
Teide H	ODG29A-1	1493.2	21.37	68.42	10.21
Teide H	ODG29A-1	1552.8	22.98	66.74	10.28
Teide H	ODG29A-1	1627.5	23.49	67.34	9.17
Teide H	ODG29A-1	1701.1	21.43	68.12	10.45
Teide H	ODG29A-1	1718.3	21.35	68.30	10.35
Teide H	ODG29A-1	1788.8	21.98	68.15	9.88
Teide H	ODG29A-1	1872.2	23.95	67.90	8.15
Teide H	ODG29A-1	1922.4	25.31	67.96	6.73
Teide H	ODG29A-1	2005.7	26.24	65.84	7.92
Teide H	ODG29A-1	2026.5	27.77	65.52	6.71
Teide H	ODG29A-1	2101.8	45.05	52.95	2.00
Teide H	ODG29A-3	0.0	16.94	68.47	14.59
Teide H	ODG29A-3	33.4	17.65	68.60	13.75
Teide H	ODG29A-3	73.3	18.23	67.64	14.13
Teide H	ODG29A-3	133.9	23.36	67.51	9.14
Teide H	ODG29A-3	170.4	21.45	68.16	10.39
Teide H	ODG29A-3	217.9	22.32	67.92	9.76
Teide H	ODG29A-3	259.6	22.89	67.74	9.37
Teide H	ODG29A-3	277.4	22.13	68.41	9.45
Teide H	ODG29A-3	304.7	19.94	70.94	9.13
Teide H	ODG29A-7	0.0	19.69	68.01	12.30
Teide H	ODG29A-7	118.1	23.39	67.44	9.17
Teide H	ODG29A-7	248.8	21.63	67.83	10.54
Teide H	ODG29A-7	340.4	21.65	68.29	10.06
Teide H	ODG29A-7	423.4	23.20	67.11	9.70
Teide H	ODG29A-7.2	0.0	17.07	67.76	15.17
Teide H	ODG29A-7.2	477.9	19.97	67.69	12.34
Teide H	ODG29A-7.2	1015.2	25.47	65.99	8.54
Teide H	ODG29A-7.2	1384.1	23.85	67.53	8.62
Teide H	ODG29A-7.2	1662.1	22.32	68.04	9.64
Teide H	ODG29A-7.2	1922.7	21.21	68.21	10.57
Teide H	ODG29A-7.2	2178.9	21.92	68.16	9.92
Teide H	ODG29A-7.3	0.0	22.61	67.82	9.57
Teide H	ODG29A-7.3	51.6	20.77	67.22	12.01
Teide H	ODG29A-7.3	129.6	17.85	68.36	13.79
Teide H	ODG29A-7.3	187.0	19.63	69.77	10.61
Teide H	ODG29A-7.3	359.2	20.77	68.46	10.77
Teide H	ODG29A-7.3	431.8	20.97	68.48	10.55
Teide H	ODG29A-7.3	510.2	19.51	68.43	12.05
Teide H	ODG29A-7.3	622.3	19.45	67.86	12.69
Teide H	ODG29A-7.3	685.6	42.08	55.48	2.44
Teide H	ODG29A-7.3	718.9	41.54	55.77	2.69
Teide H	ODG29A-4.1	0.0	22.59	68.09	9.32
Teide H	ODG29A-4.1	55.5	23.66	67.46	8.88
Teide H	ODG29A-4.1	206.5	15.58	68.71	15.71
Teide H	ODG29A-4.1	322.8	19.04	68.13	12.83
Teide H	ODG29A-4.1	414.5	17.83	68.14	14.03
Teide H	ODG29A-4.1	617.9	17.70	68.02	14.27
Teide H	ODG29A-4.1	726.7	18.28	69.36	12.36
Teide H	ODG29A-4.1	830.2	17.80	68.50	13.70
Teide H	ODG29A-4.1	899.3	17.48	69.66	12.85
Teide H	ODG29A-4.1	946.0	22.16	67.15	10.69
Teide H	ODG29A-4.1	1078.6	25.28	66.09	8.63
Teide H	ODG29A-4.1	1184.2	23.11	67.42	9.47
Teide H	ODG29A-4.1	1253.4	15.78	69.07	15.15
Teide H	ODG29A-4.1	1305.0	25.85	65.68	8.48
Teide H	ODG29A-4.1	1387.5	24.23	66.57	9.20
Teide H	ODG29A-4.1	1467.5	25.18	66.30	8.52
Teide H	ODG29A-4.1	1522.8	25.52	66.00	8.48
Teide H	ODG29A-4.1	1606.8	24.90	66.68	8.41
Teide H	ODG29A-4.1	1645.6	17.44	70.42	12.14
Teide H	ODG29A-4.1	3005.8	18.53	68.16	13.31
Teide H	ODG29A-4.1	3128.2	17.66	68.19	14.14
Teide H	ODG29A-4.1	3247.2	22.58	68.08	9.34
Teide H	ODG29A-4.1	3329.4	21.70	66.80	11.50

Teide H	ODG29A-4.1	3419.0	20.39	68.06	11.55
Teide H	ODG29A-4.1	3479.7	18.92	68.58	12.50
Teide H	ODG29A-4.1	3540.3	25.56	66.46	7.98
Teide H	ODG29A-4.1	3631.8	23.39	67.24	9.38
Teide H	ODG29A-4.1	3701.5	23.50	66.78	9.72
Teide H	ODG29A-4.1	3760.1	21.90	67.94	10.16
Teide H	ODG29A-4.1	3835.2	21.22	68.27	10.51
Teide H	ODG29A-4.1	3895.6	19.39	69.45	11.16
Teide H	ODG29A-4.2	0.0	13.60	71.65	14.75
Teide H	ODG29A-4.2	24.3	18.29	69.37	12.34
Teide H	ODG29A-4.2	27.0	19.97	68.50	11.53
Teide H	ODG29A-4.2	83.6	21.72	67.30	10.98
Teide H	ODG29A-4.2	116.3	18.58	66.33	15.09
Teide H	ODG29A-4.2	142.6	15.84	70.11	14.05
Teide H	ODG29A-4.2	147.5	17.83	68.99	13.18
Teide H	ODG29A-4.2	438.0	20.94	65.42	13.64
Teide H	ODG29A-4.2	454.7	20.31	68.39	11.29
Teide H	ODG29A-4.2	496.7	9.92	71.81	18.27
Teide H	ODG29A-4.2	524.4	29.21	64.38	6.41
Teide H	ODG29A-4.2	541.9	14.94	70.01	15.05
Teide H	ODG29A-4.2	545.1	17.60	68.39	14.01
Teide H	ODG29A-6	0.0	21.48	68.35	10.16
Teide H	ODG29A-6	76.6	25.56	66.56	7.88
Teide H	ODG29A-6	117.3	23.16	66.87	9.97
Teide H	ODG29A-6	164.0	20.39	68.04	11.57
Teide H	ODG29A-6	252.2	21.91	67.12	10.98
Teide H	ODG29A-6	365.5	21.56	68.30	10.14
Teide H	ODG29A-6	415.0	19.85	69.37	10.79
Teide H	ODG29A-8	0.0	20.47	69.10	10.43
Teide H	ODG29A-8	16.6	39.41	55.26	5.33
Teide H	ODG29A-8	43.5	21.33	67.87	10.80
Teide H	ODG29A-8	122.8	18.83	68.29	12.88
Teide H	ODG29A-8	188.6	17.88	67.73	14.39
Teide H	ODG29A-8	232.5	16.02	69.87	14.11
Teide H	ODG29A-8	259.6	17.50	68.67	13.82
Teide H	ODG29A-8	290.4	19.11	67.97	12.92
Teide H	ODG29A-8	351.1	26.22	64.70	9.09
Teide H	ODG29A-8	376.9	23.56	66.36	10.08
Teide H	ODG29A-8	411.5	24.28	65.95	9.77
Teide H	ODG29A-8	455.9	16.52	73.27	10.21
Teide H	ODG29A-8	480.9	46.43	50.72	2.85
Teide H	ODG29A-8.2	0.0	20.50	68.08	11.42
Teide H	ODG29A-8.2	15.9	19.94	68.99	11.08
Teide H	ODG29A-8.2	32.2	17.66	67.54	14.81
Teide H	ODG29A-8.2	50.0	13.36	68.38	18.26
Teide H	ODG29A-8.2	64.4	19.96	68.87	11.16
Teide H	ODG29A-8.2	75.2	21.43	68.72	9.85
Teide H	ODG29A-8.2	83.9	18.20	66.59	15.20
Teide H	ODG29A-8.2	95.9	16.67	65.90	17.43
Teide H	ODG29A-8.2	107.1	16.61	67.18	16.21
Teide H	ODG29A-8.2	127.9	15.84	69.82	14.34
Teide H	ODG29A-8.2	145.5	21.04	67.87	11.09
Teide H	ODG29A-8.2	153.2	20.33	68.15	11.52
Teide H	ODG29A-8.2	163.0	19.12	69.61	11.27
Teide H	ODG29A-8.2	172.7	17.43	74.38	8.18
Teide H	ODG29A-8.2	373.5	44.23	54.07	1.71
Teide H	ODG29A-8.2	387.2	18.37	70.31	11.32
Teide H	ODG29A-8.2	404.6	18.67	68.62	12.71
Teide H	ODG29A-8.2	414.1	18.25	69.66	12.09
Teide H	ODG29A-8.2	423.4	18.24	69.36	12.39
Teide H	ODG29A-8.2	432.8	20.33	68.44	11.23
Teide H	ODG29A-8.2	481.2	17.76	69.49	12.74
Teide H	ODG29A-8.2	488.3	18.56	68.82	12.62
Teide H	ODG29A-8.2	501.0	18.91	68.86	12.23
Teide H	ODG29A-8.2	521.5	20.04	67.97	11.99
Teide H	ODG29A-8.2	537.1	19.66	68.54	11.80
Teide H	ODG29A-8.2	559.9	19.41	69.17	11.42
Teide H	ODG29A-8.2	586.0	20.79	67.86	11.35
Teide H	ODG29A-8.2	604.3	20.61	68.14	11.25
Teide H	ODG29A-8.2	629.0	20.04	68.67	11.30
Teide H	ODG29A-8.2	658.2	19.04	68.63	12.34
Teide H	ODG29A-8.2	667.3	20.27	68.28	11.45
Teide H	ODG29A-8.2	696.5	20.90	68.27	10.83
Teide H	ODG29A-8.2	713.3	20.83	69.05	10.12
Teide H	ODG29A-8.2	773.1	21.02	67.64	11.34
Teide H	ODG29A-8.2	802.7	20.72	68.44	10.84
Teide H	ODG29A-8.2	831.3	19.65	67.89	12.46
Teide H	ODG29A-8.2	853.8	19.93	68.32	11.74
Teide H	ODG29A-8.2	864.5	19.61	68.68	11.71
Teide H	ODG29A-8.2	874.5	18.04	68.99	12.97

Teide H	ODG29A-8.2	935.4	43.82	54.24	1.94
Teide H	ODG29A-8.2	948.9	39.07	60.41	0.52
Teide H	ODG29A-9	0.0	20.50	69.44	10.06
Teide H	ODG29A-9	27.2	20.54	66.99	12.46
Teide H	ODG29A-9	61.6	22.56	67.29	10.15
Teide H	ODG29A-9	120.1	21.34	67.78	10.88
Teide H	ODG29A-9	153.9	21.60	67.49	10.91
Teide H	ODG29A-9	180.1	18.73	69.09	12.18
Teide H	ODG29A-9	230.7	22.96	68.22	8.82
Teide H	ODG29A-9	262.8	23.99	66.91	9.09
Teide H	ODG29A-9	317.0	25.55	66.52	7.93
Teide H	ODG29A-9	349.2	24.76	66.79	8.44
Teide H	ODG29A-9	383.9	22.43	67.67	9.90
Teide H	ODG29A-9	440.0	22.58	67.77	9.65
Teide H	ODG29A-9	500.7	22.40	68.46	9.14
Teide H	ODG29A-9	530.6	22.39	68.60	9.01
Teide H	ODG29A-9	580.1	23.28	69.14	7.58
Teide H	ODG29A-9	620.6	21.66	67.97	10.36
Teide H	ODG29A-9	646.3	22.29	67.88	9.83
Teide H	ODG29A-9	699.5	22.16	68.54	9.29
Teide H	ODG29A-9	749.7	21.85	67.94	10.21
Teide H	ODG29A-9	773.3	21.66	67.18	11.16
Teide H	ODG29A-9	821.3	21.65	68.32	10.03
Teide H	ODG29A-9	1524.4	17.30	69.56	13.14
Teide H	ODG29A-9	1567.9	20.91	68.11	10.98
Teide H	ODG29A-9	1641.8	23.33	67.41	9.26
Teide H	ODG29A-9	1673.9	23.03	67.05	9.92
Teide H	ODG29A-9	1737.2	22.93	67.65	9.42
Teide H	ODG29A-9	1791.5	24.12	66.40	9.47
Teide H	ODG29A-9	1886.0	22.76	67.70	9.54
Teide H	ODG29A-9	1932.5	43.26	54.47	2.27
Teide H	ODG29A-9	2024.4	23.87	67.50	8.63
Teide H	ODG29A-9	2061.3	25.87	66.31	7.82
Teide H	ODG29A-9	2124.8	25.91	66.57	7.52
Teide H	ODG29A-9	2164.1	24.61	67.25	8.14
Teide H	ODG29A-9	2241.3	23.24	67.64	9.11
Teide H	ODG29A-9	2264.3	19.59	68.45	11.97
Teide H	ODG29A-9	2331.2	20.83	67.82	11.35
Teide H	ODG29A-9	2402.9	21.95	67.22	10.83
Teide H	ODG29A-9	2490.2	20.29	67.62	12.09
Teide H	ODG29A-9	2560.3	21.81	67.45	10.75
Teide H	ODG29A-9	2627.1	25.17	66.19	8.64
Teide H	ODG29A-9	2659.4	22.80	67.27	9.92
Teide H	ODG29A-9	2717.4	23.09	66.68	10.23
Teide H	ODG29A-9	2800.1	22.24	67.66	10.11
Teide H	ODG29A-9	2835.2	36.50	60.07	3.43
Teide H	ODG29A-9	2888.9	44.48	52.40	3.12
Teide H	ODG29A-9	3929.2	42.34	55.62	2.05
Teide H	ODG29A-9	3964.0	22.97	67.23	9.80
Teide H	ODG29A-9	4013.2	21.84	67.82	10.34
Teide H	ODG29A-9	4077.6	21.54	67.53	10.93
Teide H	ODG29A-9	4124.7	20.68	67.81	11.51
Teide H	ODG29A-9	4179.5	20.74	67.79	11.47
Teide H	ODG29A-9	4258.9	21.44	67.89	10.68
Teide H	ODG29A-9	4331.5	22.29	67.28	10.44
Teide H	ODG29A-9	4383.8	23.24	66.11	10.66
Teide H	ODG29A-9	4408.8	22.62	67.38	10.00
Teide H	ODG29A-9	4450.9	27.00	64.22	8.78
Teide H	ODG29A-9	4494.1	16.74	79.57	3.69

SUPPLEMENTARY REFERENCES

Andújar, J., and Scaillet, B., 2012, Experimental Constraints on Parameters Controlling the Difference in the Eruptive Dynamics of Phonolitic Magmas: the Case of Tenerife (Canary Islands): Journal of Petrology, v. 53, p. 1777–1806, https://doi.org/10.1093/petrology/egs033.

Blundy, J., and Wood, B., 1994, Prediction of crystal-melt partition coefficients from elastic moduli: Letters to Nature, v. 372, p. 452–454, https://doi.org/10.1038/372452a0.

Fabbrizio, A., Schmidt, M., Gunther, D. and Eikenberg, J., 2009, Experimental Determination of Ra Mineral/melt Partitioning for Feldspars and ^{226}Ra-disequilibrium Crystallization Ages of Plagioclase and Alkali Feldspars: EPSL, v. 280, p. 137-148.

Icenhower, J. and London, D., 1996, Experimental Partitioning of Rb, Cs, Sr and Ba between Alkali Feldspar and Peraluminous Melt: American Mineralogist, v. 81, p. 719–734.

Long, P.E., 1978, Experimental Determination of Partition Coefficients for Rb, Sr and Ba between Alkali Feldspar and Silicate Liquid: Geochim. Cosmochim. Acta, v. 42, p. 833–846.

Ramos, F.C., and Tepley, F.J., 2008, Inter- and Intracrystalline Isotopic Disequilibria: Techniques and Applications: Reviews in Mineralogy and Geochemistry, v. 69, p. 403–443, https://doi.org/10.2138/rmg.2008.69.11.

Ramos, F.C., and Rosenberg, P.E., 2012, Age and origin of quartz-carbonate veins associated with the Coeur D'Alene mining district, Idaho and Western Montana: Insights from isotopes and rare-earth elements: Economic Geology, v. 107, p. 1321–1339, https://doi.org/10.2113/econgeo.107.6.1321.

Ramos, F.C., Heizler, M.T., Buettner, J.E., Gill, J.B., Wei, H.Q., Dimond, C.A., and Scott, S.R., 2016, U-series and $^{40}Ar/^{39}Ar$ ages of Holocene volcanic rocks at Changbaishan volcano, China: Geology, v. 44, p. 511–514, https://doi.org/10.1130/G37837.1.

Ramos, F.C., Wolff, J.A., Buettner, J.E., Wei, H.Q., and Xu, J., 2019, Ra/Th ages of sanidine in young trachytes erupted at Changbaishan Volcano, China: Journal of Volcanology and Geothermal Research, v. 374, p. 226–241, https://doi.org/10.1016/j.jvolgeores.2019.02.006.